Fermi National Accelerator Laboratory

FERMILAB-Pub-82/19-THY
February, 1982

An Asymptotic Dispersion Relation for the Six-Particle Amplitude

HENRY P. STAPP
Lawrence Berkeley Laboratory, Berkeley, CA 94720

and

ALAN R. WHITE
Fermi National Accelerator Laboratory
P.O. Box 500, Batavia, IL 60510

(Received

ABSTRACT

The concept of an asymptotic dispersion relation associated with multi-Regge asymptotic behaviour is introduced. A particular example for the six-particle amplitude is derived in detail. In this example there are forty-four distinct spectral contributions, each of which is expressed as a triple integral over physical region invariant variables. The integrands are just the corresponding invariant dispersion denominators together with three-fold discontinuities which are expressed as integrals of physical scattering functions and their conjugates.

Operated by Universities Research Association Inc. under contract with the United States Department of Energy

2. Introduction

Experience with quantum electrodynamics suggests that the divergence problems of quantum chromodynamics will be resolved only by making incisive use of the principles of Lorentz invariance, unitarity and analyticity. These principles are formally satisfied by the individual terms of the QCD renormalized perturbation expansion, but the severity of the mass-shell infra-red divergences is generally thought to require a non-perturbative formalism to define the theory. On the other hand, non-perturbative approaches which seem to have the most potential for explicit calculation such as bag models and lattice theories disrupt the basic principles mentioned above and hence may not yield a satisfactory resolution to the divergence problems.

Dispersion relations provide a well-structured non-perturbative framework that retains the properties of Lorentz invariance, unitarity and analyticity. In the context of non-abelian gauge theories (with the Higgs mechanism operating) these relations have been found to provide a highly efficient and practical way of generating, in reorganized form, the asymptotically dominant (leading log) contributions of perturbation theory at high energy. One may see this by comparing, for example, the sixth and eighth order calculations of Lipatov et al.[1] with the more traditional Feynamn diagram calculations.[2]

But beyond this matter of practical expediency dispersion relations have the important virtue that they can naturally incorporate the general property of Regge asymptotic behaviour. Thus especially and particularly in the area of asymptotic behaviour the dispersion relations provide a natural vehicle with which to approach the problems of QCD. Since the perturbative calculations with massive (Higgs mechanism) gluons indeed lead to Regge asymptotic behaviour, a general multi-Regge formalism can be combined with the dispersion relations to formally sum infinite numbers of perturbative terms. Combining this procedure with the massless limit one obtains a framework in which the principles of Lorentz invariance, analyticity and unitarity are used to sum infinite sets of infra-red divergent QCD perturbation theory diagrams.

It has recently been shown[3] by one of us (A.R.W.) that the mass-shell infra-red divergences of QCD can be successfully controlled and analyzed within this framework. The analysis leads directly to confinement and to chiral symmetry breaking, with high-energy diffractive scattering shown to depend significantly on both the gauge group and the fermion content of the theory. The consequent connection between QCD and the Reggeon Field Theory Critical Pomeron makes the experimental measurement of diffraction scattering at $\bar{p}$-p collider energies potentially very significant.[4]

The dispersion relations developed in the sixties were useful in certain special contexts, but proved inadequate as a practical basis for dynamics. The two principal difficulties with those earlier dispersion relations were first the break-down of two (or more) variable dispersion relations of Mandelstam type when Regge trajectories were infinitely rising and second the occurrence of complex domains of integration. This second difficulty involved not only the practical difficulty of dealing with complicated formulas for these complex regions, but the further and deeper problem that some of the functions occurring in the discontinuity formulas must be evaluated on unphysical sheets. Unphysical sheets are fraught with uncertainities and any attempt to make serious use of them has always seemed impractical.

These technical difficulties can apparently be largely, if not completely, circumvented if one is specificaly interested in the question of the dominant Regge behaviour in certain multi-Regge regimes of phase-space and, accordingly, designs dispersion relations to display precisely these particular terms. Many-variable dispersion relations are certainly needed for this purpose. However, the problem with infinitely rising Regge trajectories is avoided by using a many-variable generalization of the earlier fixed-t dispersion relations instead of many-variable dispersion relations of the Mandelstam type. Fixing generalized "t-variables" and certain other variables has the important added effect of burying many of the most troublesome singularities in inaccessible regions. In addition most, and very possibly all, of the remaining complex singularities appear to be eliminated by going to the asymptotic regime. The resulting "asymptotic dispersion relations" were first introduced by us in Ref. 5.

Our original description of the asymptotic dispersion relations was both abstract and brief. Many details crucial for their application were not given. In view of the above-mentioned applications to QCD it seems now appropriate to set forth a more detailed account. We begin on a concrete note by giving here a complete description of the asymptotic dispersion relation in a particular case. This case is sufficiently complicated to illustrate the general ideas, yet sufficiently simple to be easily described in full. It is the case of the six-particle amplitude in a particular multi-Regge region. In this case all the needed multiple discontinuity formulae have been derived both from physical region S-Matrix methods[7] and from Axiomatic Field Theory.[7]

This paper is intended to be self-contained. A reader wishing to understand the applications that have been made to QCD can begin here.

To explain the general concept of an "asymptotic dispersion relation" let us consider the long-established, fixed momentum transfer, dispersion relation for a four-particle amplitude A(s,t) that describes the scattering of two spinless particles. The analyticity property most immediately derived from field theory[8] is this: for fixed spacelike t and sufficiently large s the function A is analytic in the "cut-plane." That is A(s,t) has a domain of analyticity D:

$$D = \{|s|>s_0,\ \mathrm{Im}\ s \neq 0,\ t \text{ fixed} < 0\}. \tag{1.1}$$

Therefore applying the Cauchy formula to the contour shown in Fig. 1.1 one obtains

$$A(s,t) = \frac{1}{2\pi i}\int_{I_+} \frac{ds'\Delta(s',t)}{(s'-s)} + \frac{1}{2\pi i}\int_{I_-} \frac{ds'\Delta(s',t)}{(s'-s)} + \frac{1}{2\pi i}\int_{|s'|=s_0} \frac{ds'A(s',t)}{(s'-s)} + \frac{1}{2\pi i}\int_{|s'|=R} \frac{ds'A(s',t)}{(s'-s)}, \tag{1.2}$$

where I_+ and I_- are respectively "right" and "left-hand" cuts

$$I_+ = \{\mathrm{Im}\ s = 0,\ s_0 < \mathrm{Re}\ s < R\}$$
$$I_- = \{\mathrm{Im}\ s = 0,\ -R < \mathrm{Re}\ s < -s_0\} \tag{1.3}$$

and $\Delta(s,t)$ is the associated discontinuity of A(s,t).

Considerable effort has been devoted to the study of the last two integrals in (1.2). Many applications of analyticity[9] depend on extending D down to small s and establishing a domain of analyticity in the neighborhood of the origin. The detailed results depend on the particular mass spectrum of the theory. The outer integral, over $|s|=R$, reflects the subtraction content of the theory. In the context of Axiomatic Field Theory it can be proved[9] that $A(s,t)$ is polynomially bounded and that at most two subtractions are required if t is suitably restricted. However, if the theory is Regge behaved and we wish to study only this behaviour then we can essentially forget about the last two integrals in (1.2) for the following well-known reasons.

Suppose that the amplitude $A(s,t)$ is Regge-behaved:

$$A(s,t) \underset{|s|\to\infty}{\sim} \beta_+(t)s^{\alpha(t)} + \beta_-(t)(-s)^{\alpha(t)} \tag{1.4}$$

Suppose also that somewhere in the interval $t_a<t<t_b$, the quantity Re $\alpha(t)$ increases through -1, then one has in the full interval

$$\frac{1}{2\pi i}\int_{|s'|=s_0} \frac{ds'A(s',t)}{(s'-s)} \underset{|s|\to\infty}{\lesssim} 0\left(\frac{1}{s}\right) \ , \ t \in \{t_a,t_b\}, \tag{1.5}$$

while in some subinterval

$$\frac{1}{2\pi i}\int_{|s'|=R} \frac{ds'}{(s'-s)} \underset{R\to\infty}{\sim} R^{\alpha(t)}\to 0, \ \text{Re}\ \alpha(t)<-1. \tag{1.6}$$

Consequently to evaluate the leading Regge behaviour of $A(s,t)$ from (1.2) one can begin with t such that Re $\alpha(t)<-1$, and first take R to infinity. This leaves only the first three integrals in (1.2). They can be analytically continued to a value of t such that Re $\alpha(t)>-1$. Then (1.5) gives a non-dominant Regge contribution. Thus one obtains an asymptotic dispersion relation

$$A(s,t) = \frac{1}{2\pi i}\int_{I_+}\frac{ds'\Delta(s',t)}{(s'-s)} + \frac{1}{2\pi i}\int_{I_-}\frac{ds'\Delta(s',t)}{(s'-s)} + A_0, \quad (1.7)$$

where the Regge behaviour of A_0 is associated with exponents $\alpha(t)\leq -1$. For this result the exact choice of s_0 in (1.7) is irrelevant.

An important feature of (1.7) is that the discontinuity $\Delta(s,t)$ can be expressed as an integral over real physical variables of a function constructed from physical scattering functions and their conjugates:

$$\Delta(s,t) = \sum_m \int d\rho_m |A_m|^2 \quad (1.8)$$

where $d\rho_m$ represents the appropriate phase-space integration measure. Note that the explicit integrals in (1.7) do contain the cuts (in the s-plane) which the Regge behaviour (1.4) explicitly exhibits.

The aim of this paper is to describe a generalization of (1.7) and (1.8) to the six-particle amplitude. The explicitly displayed integrals, have real integration regions and explicitly exhibited discontinuity formulas, and are required to contain all contributions that have the cut structure required for certain multi-Regge behaviour. The residual function A_0 is required to be such that it can not contribute to the leading multi-Regge behaviour in a certain asymptotic regime. In general there will be a different asymptotic dispersion relation for each multi-Regge asymptotic regime. This is briefly discussed in Section 3 and is more fully discussed in Ref. 5.

In a gauge theory (with the Higgs mechanism operating) the presence of massive vector gluons allows the asymptotic dispersion relations to be used directly in perturbative calculations. It can be shown[1] that the leading log asymptotic behaviour of $A(s,t)$ originates from the (multi-Regge) region of the phase-space ρ_n, in (1.8), where the function A_n satisfies our multiparticle generalization of (1.7). The multi-Regge behaviour of the function A_n is a generalization of (1.4), and is generated by the multi-Regge regions of other multiple discontinuity integrals. Consequently, a perturbative (high-energy) expansion can be built up entirely through the asymptotic dispersion relations. This is essentially the program initially begun by Lipatov and co-workers,[1] and considerably advanced by Bartels.[10]

Alternatively, the complete set of asymptotic dispersion relations can be used to set up a general complex angular momentum and helicity formalism for multiparticle amplitudes. The dispersion relations are used to decompose these amplitudes into spectral components each of which can be shown to have a generalized "Froissart-Gribov" continuation of its partial-wave amplitudes.[11] These latter amplitudes then provide the basis of a (generalized) Sommerfeld-Watson representation. In addition "cross-channel" unitarity equations can be analyzed in full and a set of "reggeon unitarity" equations derived for each Froissart-Gribov amplitude. These equations allow the perturbative gauge theory calculations of Lipatov et al. to be seen as simply a building up of the Regge cut structure required by Lorentz invariance, analyticity and unitarity. These technical developments provide the basis of the QCD infra-red analysis referred to above.

The lay-out of the present paper is as follows. In Section 2 we describe a many variable generalization of Cauchy's formula known as the Bargman-Weil integral formula[12] and reduce it to a more simple form needed in the asymptotic dispersion relations. In Section 3 we briefly describe the variables used in these dispersion relations. A full description is given in Appendix A. Section 4 contains the application of the Bargman-Weil formula to the six-particle amplitude. In that Section we consider only the terms arising from the normal-threshold cut structure. This structure leads to a total of forty-four "spectral functions" in the dispersion relation. In Section 5 we discuss the Steinmann relations and the way in which a certain class of complex cuts gets buried. Finally in Section 6 we discuss in general how complex singularities and added contributions are eliminated by passing to the asymptotic regime. Reasons are given for believing that the displayed integrals of Section 4 give all the contributions that can contribute to the multi-Regge behaviour but no rigorous claim is made. Appendix A contains detailed kinematic formulas, and Appendix B contains the required discontinuity formulas.

In this paper we shall discuss neither the applications of the dispersion relation, nor its generalization to higher amplitudes, or even the diagrammatic notation of hexagraphs used to count spectral contributions. Some discussion of these points can be found in Ref. 4 and Ref. 5. However, we hope to extend the detailed account begun in the present paper to these topics in the near future.

2. THE BARGMAN-WEIL INTEGRAL FORMULA

The dispersion relation that we derive in this paper, together with its generalization to higher-order amplitudes described in Ref. 5, is based on a many-variable generalization[12] of the Cauchy integral formula. This "Bargman-Weil integral formula" allows one to express a function of n complex variables that is analytic in a domain bounded by smooth boundaries (of a certain kind) as a sum of integral contributions. Each contribution is an integral over a region of n real dimensions. The integrand is a product of n Cauchy-type denominators times the boundary-value of the function itself times a Bargman-Weil numerator function. This numerator function is a general feature of the many-variable formula and it is not uniquely defined. Certain special properties of our particular case will allow us to eliminate this numerator function and thus obtain simple uniquely defined formulae as our end result.

We now describe the Bargman-Weil formula. The form we give is not the most general one possible but it is sufficient for our purposes. Suppose a function $f(z)=f(z_1,\ldots,z_n)$ is analytic in a domain D that consists of the entire space $\mathbb{C}^n$ of the n complex variables z_i minus a set of cuts $\{C_j\}$:

$$D = \{z \in \mathbb{C}^n;\ z \notin C_j,\ j=1,..,N\} . \tag{2.1}$$

Suppose that for each cut C_j there is a function $Z_j(z)$, analytic in D and C_j such that C_j is the set of points where $Z_j(z)$ is real:

$$C_j = \{z \in \mathbb{C}^n;\ \mathrm{lm}\ Z(z_j) = 0\}. \tag{2.2}$$

Suppose that the intersection of every subset of n+1 of the cuts C_j has real dimension less than n. Finally suppose that for sufficiently large R, f(z) is identically zero for $|z|>R$, where $|z|^2 = \sum_i |z_i|^2$. (This condition can always be satisfied by introducing cuts C_j that define the various sides of a large "box" and setting f(z) equal to zero outside of this box.)

Let λ be a subset of n indices of the set $(1,\ldots,N)$ and write the corresponding set of $Z_j(z)$'s as $(Z_1^\lambda(z),\ldots,Z_n^\lambda(z))$. Let I_Λ be the set of points z that lie on all of the cuts C_j, $(j\varepsilon\lambda)$ and such that the determinant $|\partial Z_j^\lambda/\partial z_i|$ is non-zero:

$$I_\lambda=\{z\varepsilon\ {}^n;\ \mathrm{lm}\ Z_j(z)=0,\ (j\varepsilon\lambda),|\partial Z_j^\lambda(z)/\partial z_i|\neq 0\} . \tag{2.3}$$

The determinant condition in (2.3) allows one to use the set of variables $X_j^\lambda=\mathrm{Re}\ Z_j^\lambda(j\varepsilon\lambda)$ as a set of local coordinates on I_λ. If $z^\lambda(Z_1,..,Z_n)$ is the local inverse mapping from the set of variables $Z_j^\lambda(z)$ to the set of variables z then at any point z of I_λ that lies on none of the other cuts C_j, $j \not\in \lambda$, one can define the n-fold multiple discontinuity

$$\Delta^\lambda(z) = \sum(-1)^{n'} f(z^\lambda(X_1^\lambda(z) \pm i0, \ldots, X_n^\lambda(z) \pm i0)), \tag{2.4}$$

where the +i0 and −i0 indicate the boundary-value, in the variables Z_j^λ, from the upper and lower half-planes respectively, n' is the number of arguments $X_j^\lambda - i0$, and the sum is our all 2^n combinations of signs in the variables $X_j^\lambda \pm i0$.

If, for each λ, the entire set of points I_λ is the image under a single continuous one-to-one mapping $z^\lambda(X_1,\ldots,X_n)$ of an n-dimensional region I_λ' in X-space then the Bargman-Weil formula asserts that for all points z in D

$$f(z) = \sum_\lambda f^\lambda(z) , \tag{2.5a}$$

where

$$f^\lambda(z) = \left(\frac{1}{2\pi i}\right)^n \int_{I_\lambda'} dX_1 \ldots dX_n \left| \partial Z^\lambda(z)/\partial z \right|^{-1}_{z=z^\lambda(X)} \cdot$$

$$\times \frac{\Delta^\lambda(z^\lambda(X))D^\lambda(z,z^\lambda(X))}{(X_1 - Z_1^\lambda(z))\ldots(X_n - Z_n^\lambda(z))} , \tag{2.5b}$$

where $D^\lambda(z,z(X))$ is the Bargman-Weil numerator function mentioned above. Note that the requirement that the multiple-discontinuity on I_λ of the function f(z) defined by (2.5) agree with the original multiple-discontinuity

$\Delta^\lambda(z^\lambda(X))$ demands, for all X in I'_λ, that

$$D^\lambda(z(X);z(X)) = \left| \partial Z^\Lambda(z)/\mu\partial z \right|_{z=z^\lambda(X)} . \tag{2.6}$$

The expression (2.5) holds also when some or all of the regions I_λ are not the images of single one-to-one mappings z^λ, but are rather the unions of images of several such mappings, provided that in such cases the sum in (2.5) runs, for each λ, over a collection of separate mappings $z^\lambda(X)$ and corresponding regions I'_λ that combine to cover exactly once all the points z of I_λ. For this result to hold it is important that if $z_1^\lambda(X)$ and $z_2^\lambda(X)$ are two such mappings and if, for some X, $z_1^\lambda(X) \neq z_2^\lambda(X)$ then

$$D^\lambda(z_2^\lambda(X), z_1^\lambda(X)) = 0 . \tag{2.7}$$

This property ensures that the contribution to (2.5) associated with a mapping $z_1^\lambda(X)$ will give no contribution to the multiple discontinuity at $z_2=z_2^\lambda(X)$ even though all the denominators in (2.5) vanish at the inverse image X of z_2. The Bargman-Weil numerator function is constructed so that it satisfies properties (2.6) and (2.7). It has, therefore, the effect of properly sorting out the contributions from the various branches $z_i^\lambda(X)$ of the inverse of $Z^\lambda(z)$ over I_λ.

The Bargman-Weil numerator $D^\lambda(z,z')$ is not uniquely defined. It can be taken to be the determinant of any array of functions $P_{ij}^\lambda(z,z')$ that satisfy

$$Z_j^\lambda(z)-Z_j^\lambda(z') = \Sigma\, P_{ji}(z,z')(z_i - z_i') \ . \tag{2.8}$$

Note that

$$P_{ji}^\lambda \ (z,z) = \frac{\partial\ Z_j^\lambda}{\partial\ z_i} \ , \tag{2.9}$$

and hence (2.6) is satisfied. If we can find a $z'\neq z$ such that $Z_i^\lambda(z')=Z_i^\lambda(z)$ $i=1,..,n$ then the columns of the matrix $P_{ji}^\lambda(z,z')$ are linearly dependent and the property (2.7) follows.

In our case the multi-valuedness of the inverse transformation associated with (2.7) does not arise. Moreover the Bargman-Weil numerator enjoys the following property:

$$D^\lambda(z',z) = D^\lambda(z,z)+(Z_1^\lambda(z')-Z_1^\lambda(z))E_1^\lambda(z',z)+\ldots$$

$$\ldots+(Z_n^\lambda(z')-Z_n^\lambda(z))E_n^\lambda(z',z), \tag{2.10}$$

where the E_i^λ $i=1,..,n$ are entire functions of z and z' (in our case polynomials). Consequently (2.5b) can be expressed in the form

$$f^\lambda(z) = \frac{1}{(2\pi i)^n}\int_{I_\lambda} \frac{dX_1\ldots dX_n\ \Delta^\lambda(z^\lambda(X))}{(X_1-Z_1^\lambda(z))\ldots(X_n-Z_n^\lambda(z))} + A_0^\lambda \ , \tag{2.11}$$

where $A_0^\lambda = \sum_{i=1}^{n} A_{0i}^\lambda$ and

$$A_{0i}^{\lambda} = \frac{1}{(2\Pi i)^n} \int_{I_\lambda} \frac{dX_1 \dots dX_n \; \Delta^\lambda(z^\lambda(X)) E_i^\lambda(z(X),z)}{|\partial z^\lambda/\partial z| \prod_{j\neq i} (X_j - Z_j^\lambda(z))} \; . \tag{2.12}$$

Each function A_{0i}^{λ} has only (n-1) Cauchy denominators and hence has a null n-fold discontinuity at $z=x=z^\lambda(x)$. Thus it does not exhibit the "maximal cut structure" characteristic of the multi-Regge behaviour with which we shall be concerned and hence can be absorbed into the term A_0 which will be the generalization of that appearing in (1.7).

3. CHOICE OF VARIABLES

The problem of what variables to use in multiparticle dispersion relations has been much discussed. The efforts to obtain mass-shell global analyticity domains from the primitive analyticity domains of field theory suggest the use of momentum variables. However, the most important singularities, namely the normal threshold branch-points, are in invariant variables. But physical-region normal-threshold branch-points are present in eleven different invariant variables for a 2-4 process and in sixteen invariant variables for a 3-3 process. Since for a six-particle amplitude there are only $3\times6-10=8$ independent variables there seems to be no completely natural set of invariant variables.

Multi-Regge theory[11,12] leads to the introduction of variables defined by sequences of Lorentz transformations. In certain physical regions these are simply sequences of rotations. Sequences of resonance production (with arbitrary spin) are naturally expressed in terms of these variables, and a general complex angular momentum theory can be developed. A detailed description of these "Toller" variables can be found in Appendix A. Here we give only a brief description together with the asymptotic forms needed to derive the asymptotic dispersion relation.

In our generalization of the "fixed-t" dispersion relation (1.7) to an n-particle amplitude a set of (n-3) momentum transfer variables t_i is kept fixed. The (n-3) variables t_i are associated one-to-one with the internal lines i of a tree diagram which we refer to as a Toller diagram (see Fig. 3.1, for example).

In general a Toller diagram consists of n external lines, one for each particle of the process, n-3 internal lines i, one for each variable t_i, and n-2 vertices. Each vertex has exactly three lines incident upon it. The variable t_i is the square of the momentum energy Q_i flowing along line i if momentum-energy is conserved at each vertex of the diagram. The remaining variables we wish to introduce are associated with sequences of Lorentz transformations that connect the rest frames of the various particles of the reaction. Such a sequence can be represented by a path in the Toller diagram that connects the lines associated with these particles.

For each external line j there is a rest frame in which the associated momentum energy vector is $p_j=(m_j,0,0,0)$. For each internal line i there is a "rest frame" in which the momentum-energy Q_i flowing along line i from left to right is $(0,0,0,+\sqrt{-t_i})$.

A path from one external line to another represents a sequence of Lorentz transformations that takes the rest frame of the first line to that of the second by passing through the rest frames of the internal lines on the path. If the momenta associated with all internal and external lines lie in the (0,3) plane then we need only those transformations z_{ij} that are boosts in the (0,3) plane from the rest frame of line i to that of line j. These boosts depend only on the t-variables and the external masses. To pass to the general case we need in addition, for each internal line i, a (0,1) boost β_i that leaves the rest frame form of Q_i unchanged, and for each vertex a (1,2) rotation w_{ij} that connects the rest frames of lines i and j.

Exact expressions for invariants as functions of the t_i, β_i and w_{ij} are given in Appendix A. For the rest of the paper we will use only the following "asymptotic" formulae. Writing $z_i=\cosh\beta_i$ then when $|z_i|\to\infty$ $\forall_i$ we have

$$2p_i\cdot p_j = c_{ij}(t,w) \prod_k f_{ijk}\, z_k + \text{terms of lower order in the } z_k \tag{3.1}$$

where the variables $t=\{t_i\}$ and $w=\{w_{ij}\}$ will be held fixed in our dispersion relation, and f_{ijk} is one if the internal line k lies on the direct path in the diagram that connects the external line i to the external line j, and is zero otherwise.

The momentum-energy vectors of the initial particles of the reaction are taken to be minus the physical energy-momentum vectors. The sign conventions for the z_i are fixed by choosing $z_i \geq 1$ to be the physical region for a particular process. For the six-particle amplitude we choose that process to be the one shown in Fig. 3.1 where the lines entering from the bottom of the diagram, that is 1 and 6, represent initial particles and those exiting from the top, that is 2,3,4 and 5, represent final particles. (We shall adopt this convention throughout this paper.) Thus the signs of the c_{ij} in (3.1) are fixed by the conditions

$$\begin{aligned} c_{ij} &> 0 \quad \text{for } i,j \in \{2,3,4,5\} \\ c_{ij} &> 0 \quad \text{for } i,j \in \{1,6\} \\ c_{ij} &< 0 \quad \text{otherwise} . \end{aligned} \tag{3.2}$$

The dispersion relation involves the entire large $|z_i|$ region. Thus the real regions of momentum-energy space generated by reversing the signs of the z_i also enter. Reversing the sign of one z_i (marked by a cross in Fig. 3.2) twists the corresponding right half of a Toller diagram by 180° relative to the left half as illustrated in Fig. 3.2. This leads to a new physical region if the particles entering from the bottom are again interpretated as initial and those emitting from the top as final. We refer to such a twist of a Toller diagram as a signature twist.

4. THE ASYMPTOTIC DISPERSION RELATION

The Bargman-Weil formula of Section 2 will now be applied to the six-particle amplitude considered as a function of the variables defined by the Toller diagram of Fig. 3.1. The variables t_1, t_2, t_3, w_{12}, w_{23} will be held fixed and so the amplitude $A(p_1,\ldots p_6)$ will be a function of z_1, z_2 and z_3 only (for simplicity we take the external particles to be spinless--the generalization of the final formula to spinning particles will be obvious). We write therefore

$$A(p(z)) = f(z) \quad , \tag{4.1}$$

were

$$f(z) = f(z_1,z_2,z_3). \tag{4.2}$$

In this Section we shall consider only the normal-threshold branch-points. The higher-order Landau singularities corresponding to triangle diagrams, box diagrams etc. will be considered in Section 6. The normal threshold cuts are defined by

$$\mathrm{Im}\ s_j = 0 \quad , \tag{4.3}$$

where s_j is the square of some sum of p_j's. Discontinuities across the cut (4.3) vanish outside of the region

$$\mathrm{Re}\ s_j > M_j^2 > 0 \quad , \tag{4.4}$$

for some "threshold" mass M_j.

For the Toller diagram of Fig. 3.1, the various possible normal threshold cuts and their asymptotic forms (up to constant coefficients) are listed below:

$$
\begin{aligned}
s_{23} &= (p_2+p_3)^2 \sim z_1 \\
s_{234} &= (p_2+p_3+p_4)^2 \sim z_1 z_2 \\
s_{24} &= (p_2+p_4)^2 \sim z_1 z_2 \\
s_{2345} &= (p_2+p_3+p_4+p_5)^2 \sim z_1 z_2 z_3 \\
s_{25} &= (p_2+p_5)^2 \sim z_1 z_2 z_3 \\
s_{245} &= (p_2+p_4+p_5)^2 \sim z_1 z_2 z_3 \\
s_{345} &= (p_3+p_4+p_5)^2 \sim z_2 z_3 \\
s_{235} &= (p_2+p_3+p_5)^2 \sim z_1 z_2 z_3 \\
s_{35} &= (p_3+p_5)^2 \sim z_2 z_3 \\
s_{34} &= (p_3+p_4)^2 \sim z_2 \\
s_{45} &= (p_4+p_5)^2 \sim z_3 \, .
\end{aligned}
\tag{4.5}
$$

There will be analagous cuts associated with the diagrams obtained by making all possible combinations of signature twists with respect to the internal lines of Fig. 3.1. Each of the cuts will have a dominant term proportional to z_1, z_2, z_3, z_1z_2, z_2z_3, or $z_1z_2z_3$. In our discussion we shall keep only these leading terms, since our intention is to obtain the dispersion relation that controls the leading asymptotic Regge behaviour. The cuts of $f(z)$ are therefore in the variables

$$Z_1(z) = z_1,\ Z_2(z) = z_2,\ Z_3(z) = z_3$$

$$Z_4(z) = z_1 z_2,\ Z_5(z) = z_2 z_3,\ Z_6(z) = z_1 z_2 z_3\ . \tag{4.6}$$

We shall define the <u>principal</u> contributions to the dispersion relation to be those with the maximal number (in our case $n-3=3$) of asymptotically distinct normal-threshold cuts. These contributions are the only ones that can lead to the 3-fold multi-Regge behaviour that we wish to use the dispersion relation to examine.

For reasons that will be explained in the following section we impose the <u>generalized Steinmann relations</u>: the multiple discontinuity across a set of cuts is required to vanish if any pair of cuts in the set define overlapping channels. (A pair of cuts define overlapping channels if and only if neither of the two complementary sets of particles defined by one cut is contained within either of the two complementary sets of particles defined by the other cut.)

The generalized Steinmann relations entail that each principal contribution corresponds to one of the following triads of asymptotic normal threshold cuts

$$z_1,\ z_1z_2,\ z_1z_2z_3 \tag{4.7a}$$

$$z_3,\ z_3z_2,\ z_1z_2z_3 \tag{4.7b}$$

$$z_2,\ z_2z_3,\ z_1z_2z_3 \tag{4.7c}$$

$$z_2,\ z_2z_1,\ z_1z_2z_3 \tag{4.7d}$$

$$z_1,\ z_3,\ z_1z_2z_3 \tag{4.7e}$$

$$z_1z_2,\ z_2z_3,\ z_1z_2z_3 \tag{4.7f}$$

$$z_2,\ z_1z_2,\ z_3z_2 \tag{4.7g}$$

Consider first the contribution of the triad (4.7a). Then using the notation of Section 2, with λ represented by a we write

$$\begin{aligned} Z_1^a(z) &= Z_1(z) = z_1 \\ Z_2^a(z) &= Z_4(z) = z_1z_2 \\ Z_3^a(z) &= Z_6(z) = z_1z_2z_3. \end{aligned} \tag{4.8}$$

Equation (2.8) then involves a set of functions $p_{ji}^a(z,x)$ that satisfy

$$\begin{aligned} (z_1-x_1) &= (z_1-x_1)\ p_{11}^a + (z_2-x_2)\ p_{12}^a + (z_3-x_3)\ p_{13}^a \\ (z_1z_2-x_1x_2) &= (z_1-x_1)\ p_{21}^a + (z_2-x_2)\ p_{22}^a + (z_3-x_3)\ p_{23}^a \\ (z_1z_2z_3-x_1x_2x_3) &= (z_1-x_1)\ p_{31}^a + (z_2-x_2)\ p_{32}^a + (z_3-x_3)\ p_{33}^a\ . \end{aligned} \tag{4.9}$$

There are many solutions, but a symmetric choice is

$$P^a_{1i} = (1,\ 0,\ 0)$$

$$P^a_{2i} = \left(\frac{1}{2}\ (z_2+x_2),\ \frac{1}{2}\ (z_1+x_1),\ 0\right)$$

$$P^a_{3i} = \left(\frac{1}{6}\ (2z_2z_3+z_2x_3+x_2z_3+2x_2x_3),\ \frac{1}{6}\ (2z_1z_3+z_1x_3+z_3x_1+2x_1x_3),\right.$$

$$\left.\frac{1}{6}\ (2z_1z_2+z_1x_2+z_2x_1+2x_1x_2)\right) \quad . \tag{4.10}$$

The determinant giving the B-W numerator is therefore

$$D^a(z,x) = \left(\frac{z_1+x_2}{12}\right)\ (2z_1z_2+z_1x_2+x_1z_2+2x_1x_2) \tag{4.11}$$

Evaluated at $z_i=x_i$ $i=1,2,3$, (4.11) gives

$$D^a(x,x) = x_1^2x_2\ , \tag{4.12}$$

Using the notation

$$(X_i^a) = (x_1, x_1x_2, x_1x_2x_3) \tag{4.13}$$

one may express the determinant in (2.5) as

$$|\partial x^a/\partial x| = x_1^2x_2 \tag{4.14}$$

which agrees with (4.12), as demanded by (2.9).

One might now try to insert (4.11) and (4.14) directly into (2.5) in order to obtain an expression for the principal contribution associated with the triad (4.7a). However, in Section 2 it was stated that we would instead use (2.11). But why is (2.11) correct and (2.5) wrong? To examine this question let us apply the original formula (2.5) to the simple function

$$f(z) = \Big[(z_1-c_1)(z_1-c_2)(z_1z_2-c_3)(z_1z_2-c_4)(z_1z_2z_3-c_5)$$

$$\times (z_1z_2z_3-c_6)\Big]^{-1} \times \prod_{i=1}^{3} \Theta(|z_i|-R) \ . \qquad (4.15)$$

One finds that in this case the powers of z in the numerator in (2.5) cause certain contributions from the combinations of the surface $|z_i|=R$ and the pole singularities to remain important even as $R\to\infty$. Superficially it might seem that f(z) has such a strong fall-off when $|z_i|=R\to\infty$ that any surface integral at infinity would be negligible. But this turns out to be true only if we exploit (2.10) and write the Bargman-Weil formula in the form (2.11).

The form (2.11) depends on the validity of (2.10). For the triad (4.7a) it can easily be checked that (2.10) holds with $D^a(z,x)$ given by (4.11): one may take (non-uniquely)

$$E_1^a = \tfrac{1}{12}(5x_1x_2-z_2x_1+z_1x_2-z_1z_2)$$

$$E_2^a = \tfrac{1}{4}\ (z_1+x_1)$$

$$E_3^a = 0\ . \qquad (4.16)$$

Thus, for the principal contribution due to, for example, the set of cuts in s_{23}, s_{234}, s_{2345} (which satisfy the generalized Steinmann relations and, according to (4.5), are of the type (4.7a)) one can write

$$f_p^a(z) = \left(\frac{1}{2\pi i}\right)^3 \int \frac{dX_1 dX_2 dX_3 \ \Delta^a(x(X))}{(X_1-Z_1^a(z))(X_2-Z_2^a(z))(X_3-Z_3^a(z))}$$

$$= \frac{1}{(2\pi i)^3} \int \frac{ds'_{23} ds'_{234} ds'_{2345} \ \Delta^a(s'_{23}, s'_{234}, s'_{2345})}{(s'_{23}-s_{23})(s'_{234}-s_{234})(s'_{2345}-s_{2345})} \tag{4.17}$$

where $s_{23}(z_1,) \sim Z_1^a(z)$, $s_{234}(z_1,z_2) \sim Z_2^a(z_1,z_2)$, $s_{2345} \sim Z_3^a(z_1,z_2,z_3)$. This formula is a simple and natural generalization of (1.7) in that it contains simple invariant denominators and in the numerator only the multiple discontinuity itself.

The same algebra and argument applies also to the triads (4.7b), (4.7c) and (4.7d). For the triad (4.4e) one has

$$D^e(z,x) = \left(\frac{z_1 z_3}{3} + \frac{z_1 x_3}{6} + \frac{x_1 z_3}{6} + \frac{x_1 x_3}{3}\right) \tag{4.18}$$

$$= D^e(x,x) + (z_1-x_1)\ \frac{1}{6}\ (z_3+2x_3) + (z_3-x_3)\ \frac{1}{6}\ (z_1+x_1) \tag{4.19}$$

Thus (2.12) holds and (2.11) gives for the principle contribution a form analogous to (4.17). The case (4.4f) is more complicated but goes through in the same way with the choice

$$D^f(z,x) = D^f(x,x)+(z_1z_2-x_1x_2)\left(\frac{1}{6}\, z_2z_3+ \frac{1}{12}\, z_2x_3-\right.$$

$$\left.- \frac{1}{12}\, x_2z_3+ \frac{1}{3}\, x_2x_3\right)$$

$$+ (z_2z_3-x_2x_3) \left(\frac{1}{6}\, z_1z_2- \frac{1}{12}\, z_1x_2 + \frac{1}{12}\, x_1z_2+ \frac{1}{3}\, x_1x_2\right)$$

$$+ (z_1z_2z_3-x_1x_2x_3) \left(- \frac{1}{4}\, z_2+ \frac{1}{4}\, x_2\right) \tag{4.20}$$

Finally, for (4.7g) one may take

$$D^g(z,x) = D^g(x,x) + (z_2-x_2) \left(\frac{1}{4}\, z_2+ \frac{3}{4}\, x_2\right), \tag{4.21}$$

and hence (2.11) can again be obtained.

The generalized Steinmann relations actually imply that each of the triads listed in (4.7) have a unique set of s_j cuts, in the physical region of Fig. 3.1, to which they correspond. They are, in the order of (4.7)

$$s_{23},\ s_{234},\ s_{2345} \tag{4.22a}$$

$$s_{45},\ s_{345},\ s_{2345} \tag{4.22b}$$

$$s_{34},\ s_{345},\ s_{2345} \tag{4.22c}$$

$$s_{34},\ s_{234},\ s_{2345} \tag{4.22d}$$

$$s_{23},\ s_{45},\ s_{2345} \tag{4.22e}$$

$$s_{24},\ s_{35},\ s_{2345} \tag{4.22f}$$

$$\text{null set} \tag{4.22g}$$

By using the triads of invariants each principal contribution can be written in the form (4.17). The particular combinations (4.22) arise because all those invariants listed are positive when all the z_i's are positive. This follows from (3.1) and (3.2).

If one reverses the signs of some z_i's one obtains a new physical region and a new set of positive invariants. For example, in the physical region given by the twisted Toller diagram of Fig. 3.2 the triads of (4.7) would correspond to the following triads of non-overlapping cuts

$$s_{23}\backsim z_1,\ s_{14}\backsim z_1(-z_2),\ s_{236}\backsim z_1(-z_2)z_3 \tag{4.23a}$$

$$s_{45}\backsim z_3,\ s_{36}\backsim(-z_2)z_3,\ s_{236}\backsim z_1(-z_2)z_3 \tag{4.23b}$$

$$\text{null set} \tag{4.23c}$$

$$\text{null set} \tag{4.23d}$$

$$s_{23}\backsim z_1,\ s_{45}\backsim z_3,\ s_{236}\backsim(z_1)(-z_2)z_3 \tag{4.23e}$$

$$s_{14}\backsim z_1(-z_2),\ s_{36}\backsim(-z_2)z_3,\ s_{236}\backsim z_1(-z_2)z_3 \tag{4.23f}$$

$$s_{365}\backsim(-z_2),\ s_{14}\backsim z_1(-z_2),\ s_{36}\backsim(-z_2)z_3 \tag{4.23g}$$

For each of the six additional physical regions obtained by further combinations of twists of the lines $i=1,2,3$ we obtain corresponding sets of non-overlapping cuts. Since they are simply obtained by twisting either the 1-line or the 3-line or both with respect to either Fig. 3.1 or Fig. 3.2 three of the regions give sets of the form (4.22) while the other three give sets of the form (4.23).

From (4.22) we obtain six principle contributions of the form (4.17) while from (4.23) we obtain five principal contributions. Altogether then we have $6\times4+5\times4=44$ principal contributions to our asymptotic dispersion relation. Thus we can write

$$A(p_1,\ldots p_6) = \sum_{\lambda} \frac{1}{(2\pi i)^3}\int \frac{ds'_{\lambda_1} ds'_{\lambda_2} ds'_{\lambda_3}\ \Delta^{\lambda}(s'_{\lambda_1},s'_{\lambda_2},s'_{\lambda_3})}{(s'_{\lambda_1}-s_{\lambda_1})(s'_{\lambda_2}-s_{\lambda_2})(s'_{\lambda_3}-s_{\lambda_3})} + A_0 \tag{4.24}$$

where the sum over λ is a sum over 44 triads of cuts in invariant variables s_{λ_1}, s_{λ_2} and s_{λ_3}. The integration regions are over real values of the s_{λ_i} and extend from some positive (but irrelevant) finite value to infinity.

In the next Section we will discuss the discontinuities that occur in (4.24) and observe that they can be expressed as products of physical scattering functions and their conjugates integrated over physical intermediate states. In Section 6 we will argue that the higher-order Landau singularites do not give any additional principal contributions.

Finally we note in passing that the non-equality encountered above of the numbers of triads of cuts associated with two physical regions related by a single twist (c.f. (4.22) and (4.23)) has the important consequence that signature properties of Regge singularities resulting from such cuts must be more complicated than those of four-particle amplitudes.

5. DISCONTINUITY FORMULAE AND GENERALIZED STEINMANN RELATIONS

The Bargman-Weil formula described in Section 2 applies to a function of n complex variables, with cuts $\mathrm{lm}\ Z_j=0$, $j=1,...$ that enjoy the property that the intersection of each subset of n+1 cuts has real dimension less than n. But all of the cuts $\mathrm{lm}\ Z_i=0$ corresponding to normal thresholds are associated with real analytic functions $Z_i(z)$. Hence they all contain the real n-dimensional set

$[z \quad ^n$: $\mathrm{lm}\ z_i=0$, $\mathrm{Re}\ z_i$ sufficiently large, $i=\{1,\ldots n\}\}$. This difficulty may be circumvented by giving each of the surfaces $\mathrm{lm}\ Z_j=0$ a small displacement in imaginary space. (The tiny piece near each normal threshold is negligible.) Replacing each Z_j by $Z_j+i\varepsilon_j$ shifts each of the cuts slightly away from the real physical region and reduces the intersection region of any n of the normal-threshold cuts to an n real dimensional region lying close to the physical region. In addition, no (n+1) of these surfaces will intersect on any n-dimensional region. This fact is illustrated in Fig. 5.1.

The original Steinmann relations[13] refer to boundary-values obtained from certain off mass-shell cones in field theory. These relations have been extended to the Generalized Steinmann relation referred to in the last Section. These generalized relations hold for certain on mass-shell functions, which can be considered to be the boundary-values from all 2^{11} sides of the eleven cuts (4.5) that enter the physical region of Fig. 3.1, and the similar boundary values corresponding to all 2^{16} sides of the sixteen normal threshold cuts entering the physical region of Fig. 3.2. These boundary values, are used to form the 3-fold multiple discontinuity functions $\Delta^{\lambda}(s_{\lambda_1}, s_{\lambda_2}, s_{\lambda_3})$ occurring in (4.24). The 3-fold discontinuities have been calculated (independently) from both field-theoretic and S-Matrix principles. They are given in Appendix B.

The functions that satisfy the generalized Steinmann relations are initially defined by "algebraic" manipulation of unitarity integrals, rather than by analytic continuation. Hence, á priori, they need not be the boundary values that occur in the dispersion relation. A thorough discussion of this question requires a consideration of the higher-order singularities and so propertly belongs in the next Section. However, it may aid in the understanding of the discontinuity formulae listed in Appendix B and also better enplain the simplification achieved by writing asymptotic dispersion relations if we give a very brief heuristic outline of the origins of the boundary value functions[6] (in the S-Matrix formalism).

Let us write the S-Matrix as $S=1+R^+$ and its hermitian conjugate as $S^+=1-R^-$. Then the unitarity equation $SS^+=1$ entails, formally, that

$$R^+ = \frac{R^-}{1-R^-} \tag{5.1}$$

$$= \sum (R^-)^n . \tag{5.2}$$

Using a conventional bubble diagram notation for R^+ and R^- and inserting intermediate states into (5.2) one obtains for all connected amplitudes (the notation is explained in detail in Appendix B)

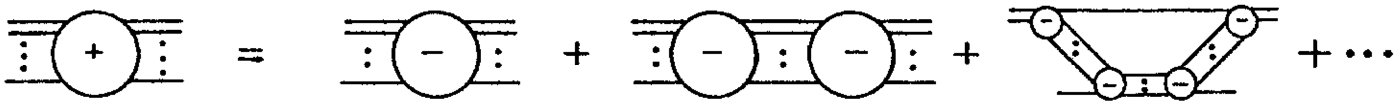

$$= \sum B^{-} \qquad (5.3)$$

(5.4)

where the sum is over all possible connected (minus) bubble diagram functions containing those intermediate state integrations allowed by the values of the external momentum variables of the 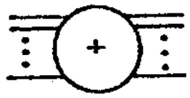 amplitude. This last amplitude is, of course, the physical region boundary-value from above all normal-threshold cuts.

The series (5.4) displays explicitly all possible normal threshold <u>and higher-order</u> Landau singularities, in the sense that new terms appear in the series whenever such a (generalized) threshold is passed. The sum of these new terms actually defines the discontinuity at such a threshold. Hence the boundary-value from underneath any particular normal threshold cut differs from 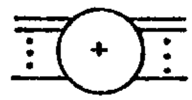, which is given by the complete sum in (5.4), by those terms in (5.4) which have a phase-space integration in the relevant channel. Extending this argument, multiple discontinuities can be defined from (5.4) by keeping only those terms which have <u>all</u> the corresponding phase-space integrations. This leads directly to the formalae quoted in Appendix B but with some exceptions. For certain "bad boundary-values" an ambiguity arises in that boundary-value functions defined by this process and the analogous process based on the hermitian conjugate version of (5.4) do not coincide. The ambiguity is directly due to bubble diagram functions that enter the series only as higher-order Landau singularities are encountered. The ambiguity can be resolved by imposing the generalized Steinmann relations and the result is the complete set of discontinuity formulae given in Appendix B.

The "bad boundary-value functions" defined by this procedure are, however, known to be boundary values of functions that, in sufficiently small neighborhoods of the physical region, are only piecewise analytic. Thus the boundary values defined in different sectors of the real region are not connected by paths of analytic continuation that remain always close to the real physical region. Prior to the introduction of the asymptotic dispersion relations they appeared unsuited for use in dispersion relations that lacked complex cuts. It is remarkable, therefore, as we discuss in the next Section, that in the asymptotic dispersion relation represented by the integrals in (4.24) the bad boundary values enter only as the boundary values of the functions defined in the three-dimensional analogs of the small triangular regions illustrated in Fig. 5.1. These regions are everywhere close to the real physical domain and they shrink to zero as the small quantities ε_j in the arguments $Z_j+i\varepsilon_j$ tend to zero. Consequently one may, in the framework of the asymptotic dispersion relations, enjoy the considerable simplifications entailed by the generalized

Steinmann relations without incurring the complications entailed by complex cuts.

Higher order Landau singularities may in principle also give complex cuts arising from their occurrence in "good boundary-value" functions. This is briefly discussed in the next Section.

6. HIGHER-ORDER SINGULARITIES

As mentioned in the introduction, a long-standing difficulty with the idea of applying many-variable dispersion relations to many-particle amplitudes has been the complications generated by the higher-order singularities associated with triangle diagrams, box diagrams etc. Many years ago Fronsdal, Norton and Mahanthappa[15] showed that a straightforward application of the Bargman-Weil theorem to scattering functions leads <u>in general</u> to complicated contributions from non-real regions of momentum space. Evaluation of the associated discontinuities requires analytic continuation of some of the amplitudes appearing in the discontinuity formulae away from their original region of definition and into unphysical sheets. These sheets are fraught with unknown dangers and difficulties, and continuation into them appears impractical. Furthermore, complex contributions far from the physical region would be likely to ruin the generalized Froissart-Gribov continuations, upon which the development of multi-Regge theory from the asymptotic dispersion relations is based.[11]

A principle virtue of the dispersion relation described above is that (apart from the generalized "subtraction term" A_0 in (4.24) which results from surfaces at infinity, and sufficiently small finite surfaces) all the three-fold discontinuities are evaluated directly in the physical region. This is automatic for the normal threshold intersections described in Section 4. But it appears to us quite likely that these will in fact be the only terms that will have the asymptotic conbination of cuts that are required for the corresponding multi-Regge behaviour.

There are two main points. The first concerns the bad boundary values referred to briefly in the last Section and defined precisely in Ref. 6. As we noted there "bad functions" have bad analytic properties. But each good function (in each real sector) has been shown to be the boundary-value of a single analytic function: the parts lying on the opposite sides of any singularity surface lying in the physical region are connected by a path of analytic continuation that makes an arbitrarily small detour around this singularity surface. In contrast the bad functions, like the bubble diagram functions from which they were constructed, have no such continuations, and hence are not boundary values of single analytic functions.

If we had to consider the cuts attached to the surfaces where the bad functions change their analytic form we would be in danger not only of disrupting the crossing properties of amplitudes (by the extension of the cuts to infinity) but also of obtaining complex contributions to our dispersion relation, with the ensuing problems already described above. If, however, we can show that the bad boundary-values are buried in the analogs of the small triangle of Fig. 5.1, as asserted in the last Section, then in the first place any contribution from the cuts involved in defining them will disappear from the integration region as the ε_j tend to zero, in the second place these contributions to the dispersion integral will, in any case, only affect the value of the function inside the little triangle and hence have no bearing at all on the function outside this region.

The bad functions are those that correspond to a boundary-value from below two $3\to3$ overlapping cuts and above two $2\to4$ (or $4\to2$) cuts, or from above the two $3\to3$ overlapping cuts and below two $2\to4$ ($4\to2$) cuts. The possible bad configurations are shown in Fig. 6.1, where either the upper signs or the lower signs must be used throughout.

Suppose first that, with the notation of Fig. 6.1, the z-variables associated with the four cuts are

$$s_1 \simeq c_{34}z_2,\ s_2 \simeq c_{35}z_2z_3$$
$$s_3 \simeq c_{24}z_1z_2,\ s_4 \simeq c_{25}z_1z_2z_3. \qquad (6.1)$$

Then

$$s_1 s_4 \simeq c\, s_2 s_3, \quad c = \frac{c_{24} c_{35}}{c_{34} c_{25}} > 0 \ , \tag{6.2}$$

where $c>0$ is implied by (3.2) (or more generally by the combination of $|\mathrm{Im}\ s_j| \simeq 0$ with the condition that $\mathrm{Re}\ s_j$ is above threshold). But (6.2) is incompatible with the sign requirements from Fig. 6.1 which are that

$$\mathrm{Im}\ s_1,\ \mathrm{Im}\ s_4 > 0;\ \mathrm{Im}\ s_2,\ \mathrm{Im}\ s_3 < 0 \ , \tag{6.3a}$$

or

$$\mathrm{Im}\ s_1,\ \mathrm{Im}\ s_4 < 0;\ \mathrm{Im}\ s_2,\ \mathrm{Im}\ s_3 > 0 \ . \tag{6.3b}$$

The incompatibility of the conditions (6.3) with (6.2) means that the region from which the boundary-value, represented by Fig. 6.1, is approached must, for sufficiently large $\mathrm{Re}\ z_i$, vanish (when the ε_j's of the proceeding Section are set to zero). The boundary value is indeed "hidden" inside a region of the form of Fig. 5.1. Thus the asymptotic dispersion relations neatly bury the regions of (complex) momentum space where the worst complex singularities occur.

Box diagrams that do not map in a planar manner onto the Toller diagram that we are considering must also be examined. For example, if the particles 3,4 and 5 of Fig. 6.1(a) are identified with particles 4,5 and 3 respectively of Fig. 3.1, then

$$s_1 \simeq C_{45}z_3,\ s_2 \simeq C_{35}z_2z_3$$

$$s_3 \simeq C_{25}z_1z_2z_3,\ s_4 \simeq C_{25}z_1z_2z_3\ . \qquad (6.4)$$

This is again incompatible with (6.3). But now the cuts in s_3 and s_4 that bound the bad boundary value region are in fact asymptotically equivalent. This means that sub-asymptotically these cuts are distinct, as illustrated in Fig. 6.2. However, the contribution of such a region to the dispersion relation would be associated with a triad that involves two asymptotically equivalent cuts. But triple-Regge asymptotic behaviour can not arise from such a triad, since this behaviour has the phase-structure of a function with three asymptotically inequivalent cuts.

The discussion of the bad boundary configurations (6.1) and (6.4) covers, in essence, all of the possibilities and hence one finds that no bad boundary value complications can occur in the principal contributions to (4.24).

The second main point to be considered when discussing complex singularities contributing to the principal contributions of (4.24) concerns the higher-order singularities occurring in the good boundary-value functions. More work is needed on this. But we think it likely that these singularities will not contribute to the asymptotic dispersion relations. For the triple discontinuity associated with the next most complicated contribution, namely that arising from two normal-threshold cuts and one triangle-diagram cut vanishes, while the singularities associated with more complex diagrams tend to be shielded by the cuts associated with less complex ones, due to the hierarchy structure. We hope to be aboe to give a detailed proof that higher-order singularities do not give principal contributions to asymptotic dispersion relations in the near future.

REFERENCES

[1] L.N. Lipatov, Sov. J. Nucl. Phys. 23, 642 (1976); V.S. Fadin, E.A. Kuraev and L.N. Lipatov, Phys. Letts. 60B, 50 (1975), Soviet Phys. JEPT 44, 443 (1976).

[2] B.M. McCoy and T.T. Wu, Phys. Rev. Letts. 35, 604 (1975); L. Tyburski, Phys. Rev. D13, 107 (1976); H. Cheng and C.Y. Lo, Phys. Rev. D13, 1131 (1976), D15, 2959 (1977).

[3] A.R. White, CERN preprint TH2976 (1980), to be published in Annals of Physics, CERN preprint TH3115 (1981), to be published in Proceedings of the Seminar on Theoretical Aspects of QCD, Marseilles (1981).

[4] A.R. White, Fermilab preprint FERMILAB-Conf-82/16-THY (1982), to be published in Proceedings of the Topical Conference on Forward Collider Physics, Madison, Wisconsin (1981).

[5] H.P. Stapp and A.R. White, Lectures at the Les Houches Institute, published by North Holland (1975).

[6] J. Coster and H.P. Stapp, J. Math. Phys. 16, 1288 (1975), see also H.P. Stapp, Ref. 5.

[7] K. Cahill and H.P. Stapp, Annals of Physics, 90, 438 (1975).

[8] J. Bros, H. Epstein and V. Glaser, Comm. Math Phys. 1, 240 (1965).

[9] A. Martin, Scattering Theory: Unitarity, Analyticity and Crossing, Lecture Notes in Physics (Springer-Verlag) (1969).

[10]J. Bartels, CERN preprint TH3153 (1981), to be published in Proceedings of the Seminar on Theoretical Aspects of QCD, Marseilles (1981).

[11]A. R. White, Ref. 5.

[12]A. Weil, Math. Ann., 11, 178 (1935); B.A. Fuks, Introduction to the Theory of Analytic Functions of Several Complex Variables, (American Math. Soc., Providence, Rhode Island, 1963).

[13]M. Toller, Nuovo Cimento 54A, 295 (1968).

[14]O. Steinmann, Helv. Phys. Acta 33, 257, 347 (1960).

[15]C. Fronsdal, R.E. Norton, and K.T. Mahanthappa, Phys. Rev. 127, 1848 (1962), J. Math. Phys. 4, 859 (1963).

APPENDIX A. ANGULAR VARIABLES

To introduce, precisely, the variables used in the text, it will suffice to define standard frames 1-6 as indicated in Fig. A1. These frames are defined as follows:

Frame 1

Q_1 lies in a rest frame, P_1 and P_2 lie in the (0,3) plane

Frame 2

Q_1 lies in a rest frame, P_3 and Q_2 lie in the (0,3) plane

Frame 3

Q_2 lies in a rest frame, P_3 and Q_2 lie in the (0,3) plane

Frame 4

Q_2 lies in a rest frame, P_4 and Q_3 lie in the (0,3) plane

Frame 5

Q_3 lies in a rest frame, P_4 and Q_2 lie in the (0.3) plane

Frame 6

Q_3 lies in a rest frame, P_5 and P_6 lie in the (0,3) plane.

We next define sets of Lorentz transformations as follows:

A. A (0,3) boost η_{ik} i=1,...6 takes particle i from its rest frame to frame k attached to the vertex where the particle line is attached.

B. (0,1) boosts β_1, β_2, β_3 transform from frames 1 to 2, 3 to 4 and 5 to 6 respectively.

C. A combination of an (1,2) rotation w_{12} (w_{23}) and a (0,3) boost ξ_{12} (ξ_{23}) transforms from frame 2 to 3 (4 to 5).

The boosts η_{ik} can be expressed in terms of masses m_i and the t_i e.g.

$$\sinh \eta_{21} = \frac{Q_1^2-m_1^2+m_2^2}{2Q_1m_2} .$$

The boosts ξ_{12}, ξ_{23} can also be expressed in terms of the m_i and the t_i e.g.

$$\cosh\xi_{12} = \frac{Q_1^2+Q_2^2+m_3^2}{2Q_1Q_2} .$$

The variables β_1, β_2, β_3, ω_{12} and ω_{23} are parameters and can be used to express any of the external momenta in any frame e.g. in frame 1

$$P_2 = (m_2\cosh\eta_{21},0,0,m_2\sinh\eta_{21}) ,$$

in frame 2

$$P_2 = (m_2\cosh\eta_{21}\cosh\beta_1,\ m_2\cosh\eta_{21}\sinh\beta_1,0,m_2\sinh\eta_{21})$$

in frame 3

$$\begin{aligned} P_2 = (&m_2\cosh\eta_{21}\cosh\beta_1\cosh\xi_{12}-m_2\sinh\eta_{21}\sinh\xi_{12} ,\\ &m_2\cosh\eta_{21}\sinh\beta_1\cos\omega_{12},m_2\cosh\eta_{21}\sinh\beta_1\sin\omega_{12},\\ &m_2\sinh\eta_{21}\cosh\xi_{12}+m_2\cosh\eta_{21}\cosh\beta_1\sinh\xi_{12}) \end{aligned}$$

in frame 4

$$
\begin{aligned}
P_2 = (&m_2\cosh\eta_{21}\cosh\beta_1\cosh\xi_{12}\cosh\beta_2 - m_2\sinh\eta_{21}\sinh\xi_{12}\cosh\beta_2 - \\
&-m_2\cosh\eta_{21}\sinh\beta_1\cos\omega_{12}\sinh\beta_2,\ m_2\cosh\eta_{21}\sinh\beta_1\cos\omega_{12}\cosh\beta_2 + \\
&+m_2\cosh\eta_{21}\cosh\beta_1\cosh\xi_{12}\sinh\beta_2 - m_2\sinh\eta_{21}\sinh\xi_{12}\sinh\beta_2, \\
&m_2\cosh\eta_{12}\sinh\beta_1\sin\omega_{12}, m_2\sinh\eta_{21}\cosh\xi_{12} + m_2\cosh\eta_{21}\cosh\beta_1\sinh\xi_{12}),
\end{aligned}
$$

and so on. To evaluate P_iP_j we simply have to transform both momenta from their rest frames to a common frame. For example, to evaluate $P_2 \cdot P_5$ we can use frame 4 where P_2 has the form given above and P_5 has a form analagous to that of P_2 in frame 3 but with $\beta_1 \to -\beta_3$, $\omega_{12} \to -\omega_{23}$, $\xi_{12} \to -\xi_{23}$. This leads to

$$
\begin{aligned}
P_2\cdot P_5 = {} & [m_2\cosh\eta_{21}\cosh\beta_1\cosh\xi_{12}\cosh\beta_2 - m_2\sinh\eta_{21}\sinh\xi_{12}\cosh\beta_2 \\
& -m_2\cosh\eta_{21}\sinh\beta_1\cos\omega_{12}\sinh\beta_2]\times[m_5\cosh\eta_{56}\cosh\beta_3\cosh\xi_{23} \\
& +m_5\sinh\eta_{56}\sinh\xi_{23}] + [m_2\cosh\eta_{21}\sinh\beta_1\cos\omega_{12}\cosh\beta_2 + \\
& m_2\cosh\eta_{21}\cosh\beta_1\cosh\xi_{12}\sinh\beta_2 - m_2\sinh\eta_{21}\sinh\xi_{12}\sinh\beta_2]\times \\
& [m_5\cosh\eta_{56}\cos\omega_{23}\sinh\beta_3] - m_2\cosh\eta_{21}\sinh\beta_1\sinh\omega_{12}\times \\
& \times m_5\cosh\eta_{56}\sinh\beta_3\sin\omega_{23} - [m_2\sinh\eta_{21}\cosh\xi_{12} + \\
& m_2\cosh\eta_{21}\cosh\beta_1\sinh\xi_{12}]\times[m_5\sinh\eta_{56}\cosh\xi_{23} - \\
& m_5\cosh\eta_{56}\cosh\beta_3\sinh\xi_{23}]
\end{aligned}
$$

$$
\xrightarrow[\substack{z_1=\cosh\beta_1\to\infty \\ z_2=\cosh\beta_2\to\infty \\ z_3=\cosh\beta_3\to\infty}]{}
\begin{aligned}
& \{[m_2\cosh\eta_{21}\cosh\xi_{12} - m_2\cosh\eta_{21}\cos\omega_{12}]\times[m_5\cosh\eta_{56}\cosh\xi_{23}] \\
& +[m_2\cosh\eta_{21}\cos\omega_{12} + m_2\cosh\eta_{21}\cosh\xi_{12}]\times[m_5\cosh\eta_{56}\cos\omega_{23}]\} \\
& \times z_1 z_2 z_3
\end{aligned}
$$

$$
= \frac{c_{25}}{2}\, z_1 z_2 z_3
$$

where $c_{25} = m_2 m_5\cosh\eta_{21}\cosh\eta_{56}[\cosh\xi_{12}\cosh\xi_{23} - \cos\omega_{12}\cosh\xi_{23} + \cosh\xi_{12}\cos\omega_{23} + \cos\omega_{12}\cos\omega_{23}]$.

Clearly any other c_{ij} can be similarly evaluated.

APPENDIX B. MULTIPLE DISCONTINUITY FORMULAE

For completeness we give here exact formulae for the triple discontinuities $\Delta^{\lambda}(s_{\lambda_1}, s_{\lambda_2}, s_{\lambda_3})$ appearing in (4.24). To do this we must introduce some notation.

For the full s-matrix we write

$S(p_1 \cdots p_m; p_{m+1}, \cdots p_n) =$ 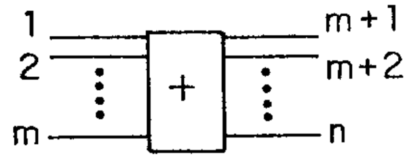 (B1)

while for s^+ we replace the + by a − and for the unit operator we replace the + by I. We make the usual cluster decomposition e.g.

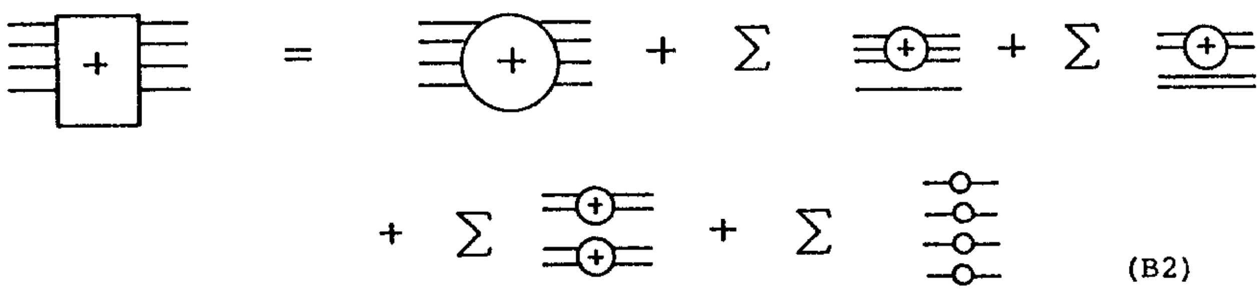

(B2)

so that a bubble represents a connected amplitude together with a momentum conservation δ-function. A phase-space integration and sum represented by a shaded strip is a unitarity sum over intermediate states e.g.

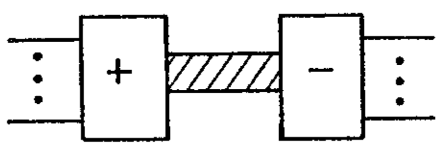

That is the strip implies a sum over all particle numbers N of intermediate lines, together with an integration or sum over all distinct sets of variables associated with these lines

$$\equiv \sum\!\!\!\!\!\!\int = \sum_{i=1}^{N} \sum_{t_i} \int \prod_{i=1}^{N} \frac{d^4P_i'}{(2\pi)^4} \, (2\pi)\delta^+(P_i'^2 - m_i^2) \, H \qquad \text{(B3)}$$

where H is the inverse of the usual symmetry number of the state. Let us further define

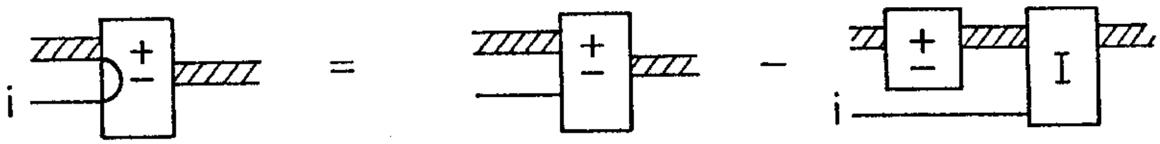

(B4)

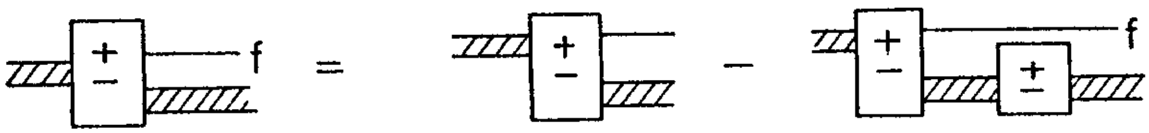

(B5)

We can now define 3-fold discontinuities as follows

$$
\begin{aligned}
\Delta(s_{\lambda_1}, s_{\lambda_2}, s_{\lambda_3}) = \; & A(\ldots s_{\lambda_1}+io, s_{\lambda_2}+io, s_{\lambda_3}+io, \ldots) \\
& -A(\ldots s_{\lambda_1}-io, s_{\lambda_2}+io, s_{\lambda_3}+io, \ldots) \\
& -A(\ldots s_{\lambda_1}+io, s_{\lambda_2}-io, s_{\lambda_3}+io, \ldots) \\
& -A(\ldots s_{\lambda_1}+io, s_{\lambda_2}+io, s_{\lambda_3}-io, \ldots) \\
& +A(\ldots s_{\lambda_1}-io, s_{\lambda_2}-io, s_{\lambda_3}+io, \ldots) \\
& +A(\ldots s_{\lambda_1}-io, s_{\lambda_2}+io, s_{\lambda_3}-io, \ldots) \\
& +A(\ldots s_{\lambda_1}+io, s_{\lambda_2}-io, s_{\lambda_3}-io, \ldots) \\
& -A(\ldots s_{\lambda_1}-io, s_{\lambda_2}-io, s_{\lambda_3}-io, \ldots)
\end{aligned}
\qquad \text{(B6)}
$$

The generalized Steinmann relations imply that this triple discontinuity is independent of the boundary values of the invariants other than $s_{\lambda_1}, s_{\lambda_2}, s_{\lambda_3}$. In a 2-4 physical region the s_{λ_i} will be a triad of the form listed in (4.22). These are of two kinds, either two 2-particle channels and the total energy, for example s_{23}, s_{45} and s_{2345} in this case

$$(2\pi)^4 \delta(\sum_i P_i)\Delta(S_{23}, S_{45}, S_{2345}) =$$

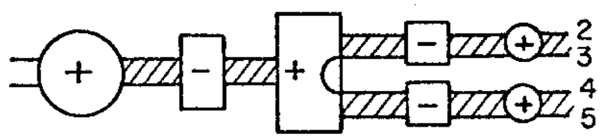

(B7)

$=$ 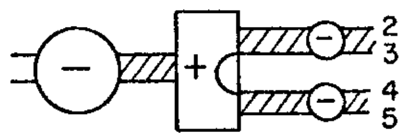

(B8)

where we define

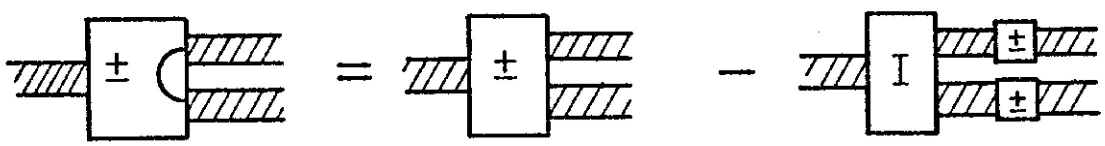

(B9)

and similarly

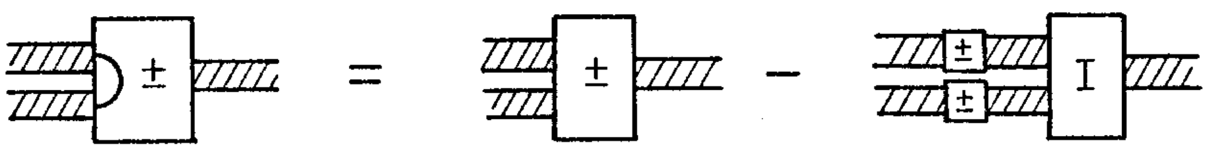

(B10)

Alternatively the three s_{λ_1} are nested, for example s_{23}, s_{234}, s_{2345} and in this case

$$(2\pi)^4\,\delta(\sum_i P_i)\,\Delta(S_{23},S_{234},S_{2345})$$

$=$ 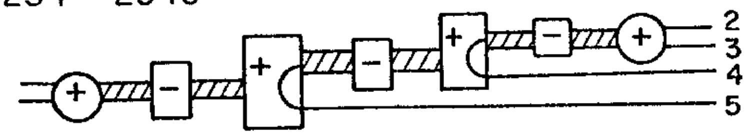

(B11)

$=$ 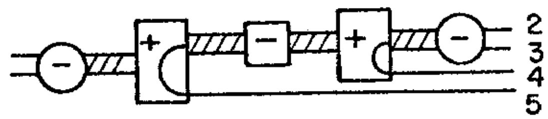

(B12)

In a 3-3 physical region the s_{λ_i} will be a triad of the form listed in (4.23). Again there are two possibilities. Both contain an initial 2-particle channel and a final 2-particle channel with either the total energy as a third invariant, for example s_{23}, s_{14} and s_{236} in which case

$$(2\pi)^4\,\delta(\sum_i P_i)\,\Delta(S_{23},S_{14},S_{236})$$

$=$ 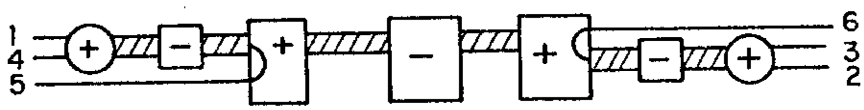

(B13)

$= -$ 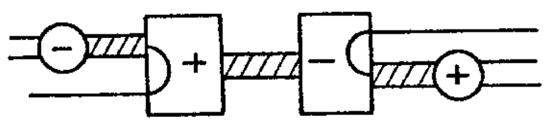
(B14)

$= -$ 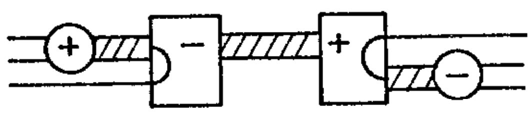
(B15)

or the third invariant is a cross-energy, for example s_{14}, s_{36} and s_{365} in which case

$$(2\pi)^4\,\delta(\sum_i P_i)\,\Delta(S_{14},S_{36},S_{365})$$

$=$ 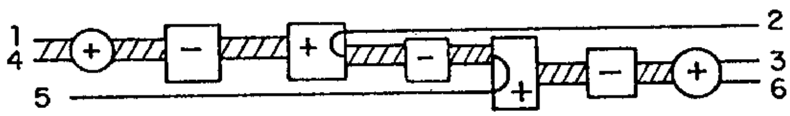 (B16)

$=$ 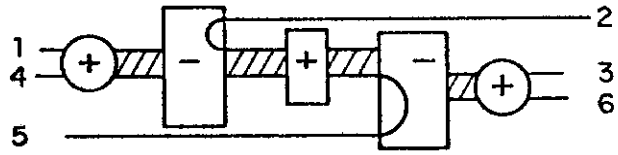 (B17)

All possible triple discontinuities needed for (4.24) are of one of the four forms (B7), (B9), (B11) or (B14). The alternative formulae given are always obtained by simple applications of unitarity.

FIGURE CAPTIONS

Fig. 1.1 The Cauchy Integration Contour for (1.2)--the Domain D is the compliment of the shaded region.

Fig. 3.1 A Toller diagram for a process with sinatemal particles.

Fig. 3.2 The reversal of the sign of z_i changes the physical region to that represented by the Toller Diagram obtained by twisting through 180° the two parts of the diagram linked by the line i.

Fig. 5.1 Three surfaces lm $2_1=0$, lm $z_2=0$ and lm $z_1+z_2=0$ intersect on the real region [z ^{2}, lm z_1=lm z_2=0}. A slight shift of each surface shifts the intersection of each pair of surfaces to a distinct 2-dimensional region.

Fig. 6.1 Bad boundary-values. The four dashed lines correspond to the cuts and the + sign (- sign) at the end of a dashed line represents the fact that the boundary value is to be taken above (below) the associated cut.

Fig. 6.2 Asymptotically equivalent cuts become distinct sub-asymptotically and expose a region associated with a bad boundary-value.

Figures
<u>SI</u>

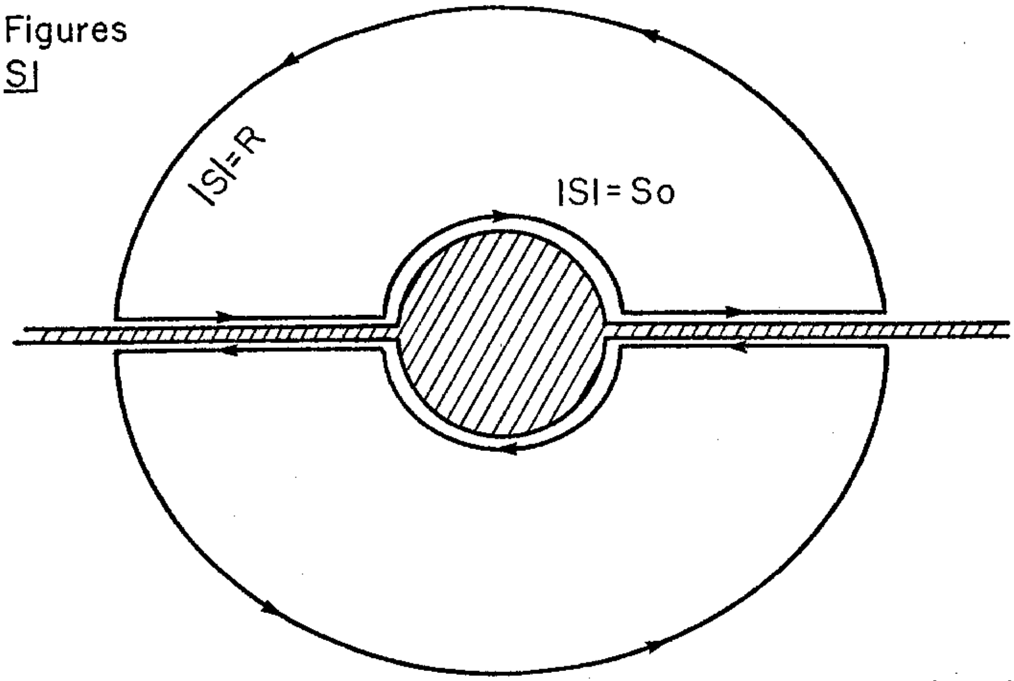

Fig. 1.1

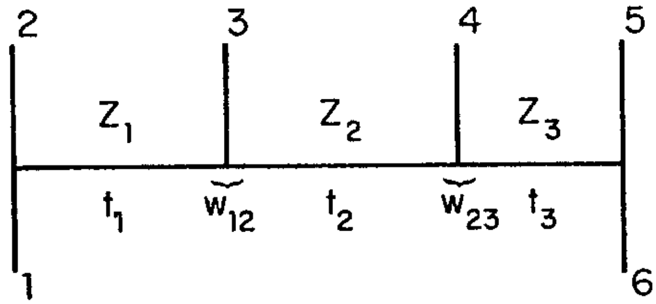

Fig. 3.1

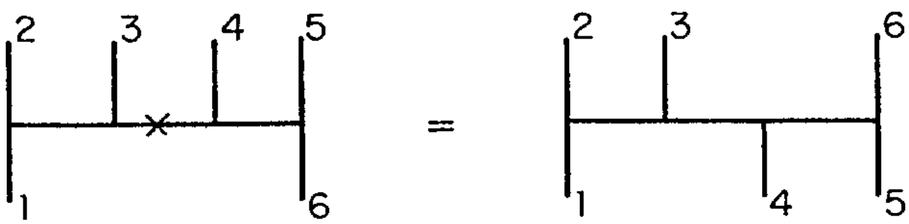

Fig. 3.2

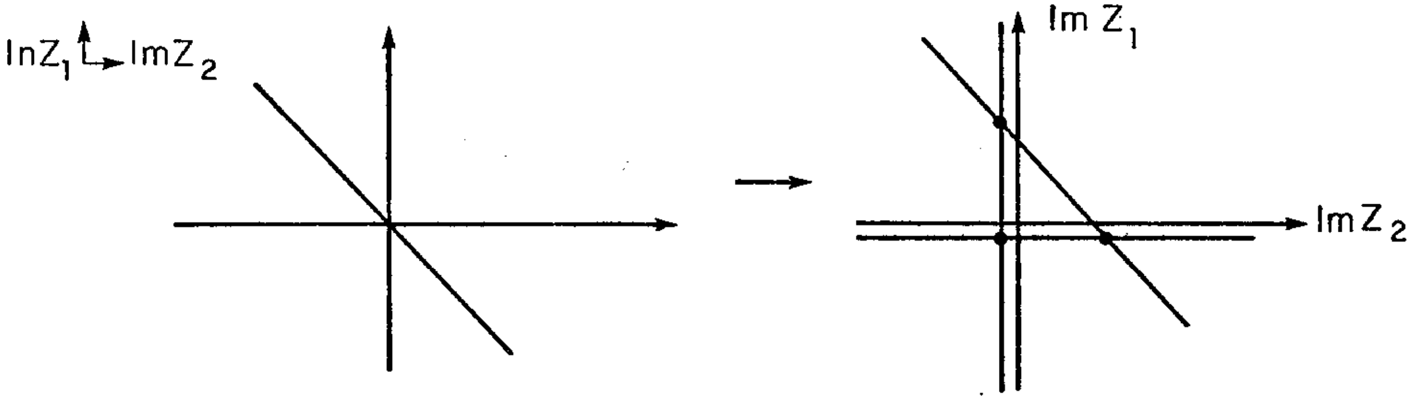

Fig. 5.1

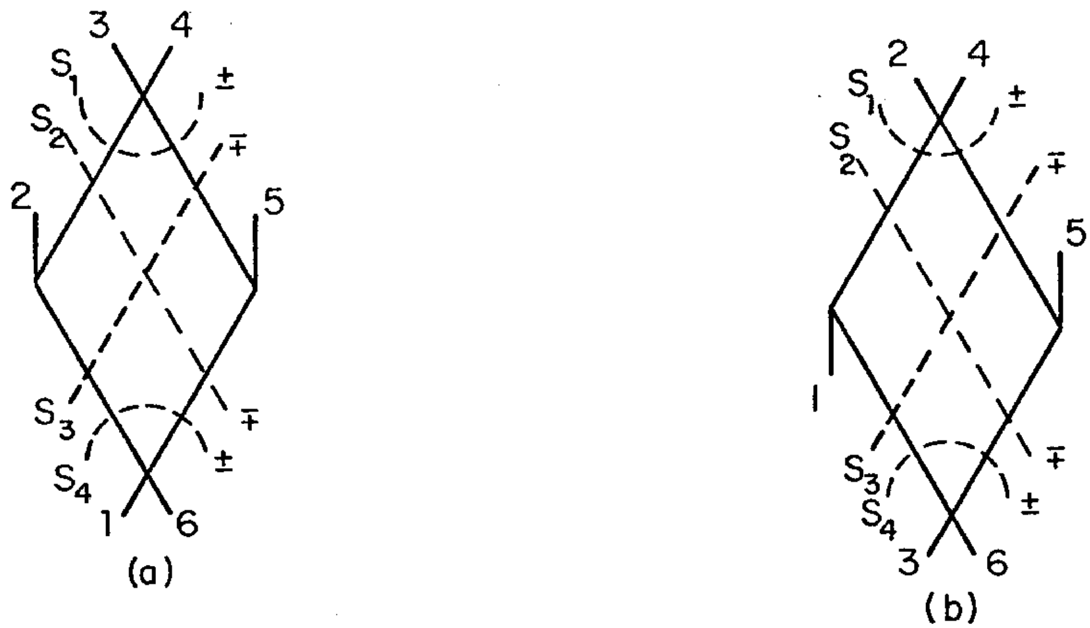

Fig. 6.1

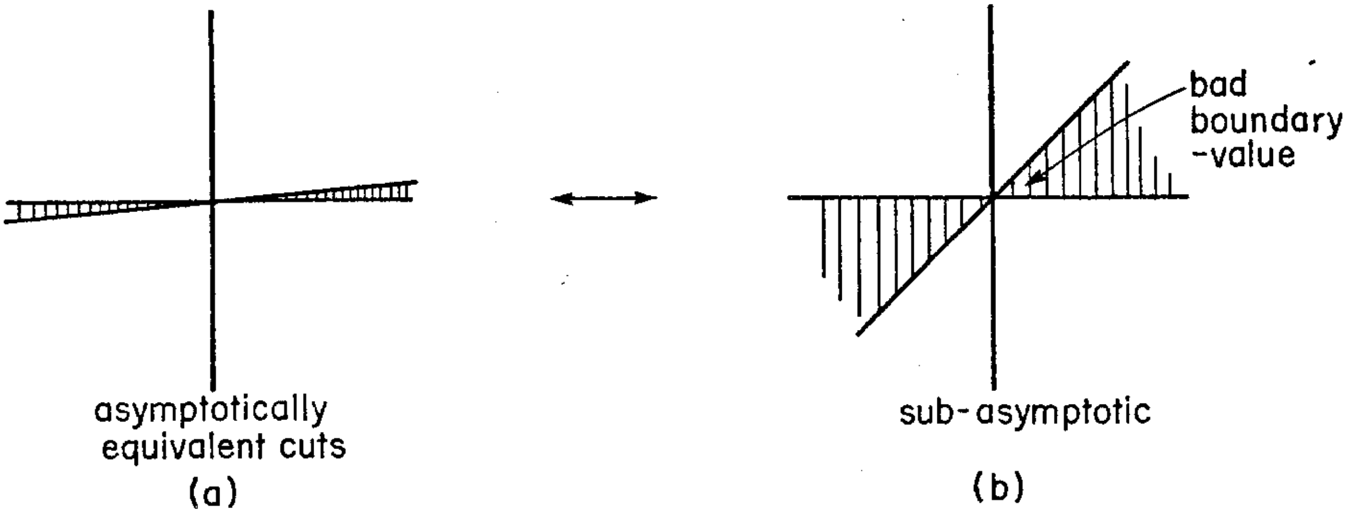
bad
boundary
-value
asymptotically
equivalent cuts
(a)
sub-asymptotic
(b)

Fig. 6.2

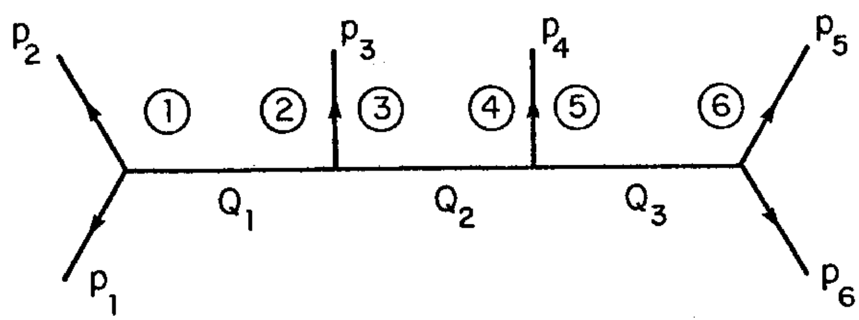
p_2
p_3
p_4
p_5
1
2
3
4
5
6
Q_1
Q_2
Q_3
p_1
p_6

Fig. A1